

QUASAR PROPER MOTIONS AND LOW-FREQUENCY GRAVITATIONAL WAVES

CARL R. GWINN,¹ T. MARSHALL EUBANKS,² TED PYNE,^{3,4} MARK BIRKINSHAW,^{3,5} AND
DEMETRIOS N. MATSAKIS²

Received 1996 November 25; accepted 1997 March 11

ABSTRACT

We report observational upper limits on the mass-energy of the cosmological gravitational wave background, from limits on proper motions of quasars. Gravitational waves with periods longer than the time span of observations produce a simple pattern of apparent proper motions over the sky, composed primarily of second-order transverse vector spherical harmonics. A fit of such harmonics to measured motions yields a 95% confidence limit on the mass-energy of gravitational waves with frequencies $\nu < 2 \times 10^{-9}$ Hz, of less than $0.11 h^{-2}$ times the closure density of the universe.

Subject headings: cosmology: observations — gravitation — quasars: general — techniques: interferometric

1. INTRODUCTION

Like variations in refractive index, the changes in space-time metric produced by gravitational waves alter optical path lengths. Propagation of light through gravitational waves preserves sources' surface brightness and total intensity, to first order in the wave amplitude (Bondi, Pirani, & Robinson 1959; Zipoy 1966; Penrose 1966), but it can produce oscillations in apparent position, at the period of the gravitational wave (Fakir 1994; Durrer 1994; Bar-Kana 1994; Pyne et al. 1996; Kaiser & Jaffe 1997). Over intervals of time much shorter than a gravitational wave period, these deflections cause a characteristic pattern of apparent proper motions (Pyne et al. 1996). In this paper, we set stringent upper limits on the energy density of such waves, using measurements of the proper motions of quasars.

Although detected only indirectly to date, most cosmologists believe that gravitational waves are commonplace. Very low frequency gravitational waves arise naturally in inflationary cosmologies (Rubakov, Sazhin, & Veriaskin 1982; Fabbri & Pollock 1983) and dominate the mass-energy of the universe in some of them (Grishchuk 1993). Other possible sources of such a background include phase transitions in the early universe, networks of cosmic strings, and collisions of bubbles (Vilenkin 1981; Hogan 1986).

Various observations set direct or indirect observational constraints on the spectrum of low-frequency gravitational radiation. These constraints are often expressed in terms of Ω_{GW} , the ratio of the mass-energy density of the gravitational waves to that required to close the universe. Some observational constraints are sensitive to a narrow range of frequencies and are best expressed in terms of the logarithmic derivative $d\Omega_{\text{GW}}/d \ln \nu$, evaluated at some frequency ν . Timing of pulsars sets observational limits for periods as great as the span of observations (Backer & Hellings 1986). For the extremely stable millisecond pulsars, the limit

corresponds to $d\Omega_{\text{GW}}/d \ln \nu < 10^{-8}$ at frequency $\nu = 4.4 \times 10^{-9}$ Hz (Kaspi, Taylor, & Ryba 1994; Thorsett & Dewey 1996). After taking into account the energy carried away by gravitational waves and the effects of Galactocentric acceleration, orbital periods of binary pulsars are sensitive to gravitational waves with periods as great as the light-travel time from the pulsar. Current limits from such data set a limit of $\Omega_{\text{GW}} h^2 < 0.04$ for 10^{-11} Hz $< \nu < 4.4 \times 10^{-9}$ Hz, and of $\Omega_{\text{GW}} h^2 < 0.5$ for 10^{-12} Hz $< \nu < 10^{-11}$ Hz (Bertotti, Carr, & Rees 1983; Taylor & Weisberg 1989; Thorsett & Dewey 1996). Here the normalized Hubble constant is $h = H_0/(100 \text{ km s}^{-1})$. A cosmological background of gravitational waves at the epoch of recombination can produce anisotropies of the cosmic background radiation (Linder 1988a; Krauss & White 1992). For gravitational wave spectra typical of inflation, the anisotropy detected by *COBE* yields a limit of $d\Omega_{\text{GW}}/d \ln \nu \leq 10^{-11}$, with sensitivity of the measurement concentrated near $\lambda \approx 2$ Gpc, or $\nu \approx 10^{-17}$ Hz (Bar-Kana 1994). Figure 1 shows these constraints graphically, along with our result, discussed below. Linder (1988b) found that a gravitational wave background in this frequency range would affect the galaxy-galaxy correlation function, but robust calculations would require knowledge of the "true" correlation function, observable only in the absence of such a background.

In contrast to these techniques, proper motions of extragalactic radio sources are sensitive to waves of arbitrarily long wavelength and are independent of the spectrum and source of gravitational wave radiation. Under the assumption that the spectrum of gravitational waves is stochastic, the squared proper motion of distant sources, suitably averaged over the sky, is proportional to the energy density of the waves, at frequencies from the inverse of the period of observation to the Hubble time.

In a previous paper (Pyne et al. 1996), we discussed the pattern of apparent proper motions of distant radio sources produced by a gravitational wave. We use the assumption that the wavelength is short compared with the distance to the source, and the adiabatic approximation that the wavelength is less than the Hubble length; however, because the observed effect is local to Earth, these assumptions can probably be relaxed without much change in the result. The best present measurements of proper motions attain accuracies of a few microarcseconds per year (Eubanks et al.

¹ Department of Physics, Broida Hall, University of California at Santa Barbara, Santa Barbara, CA 93106.

² US Naval Observatory, 3450 Massachusetts Avenue, Washington, DC 20392.

³ Harvard-Smithsonian Center for Astrophysics, 60 Garden Street, Cambridge, MA 02138.

⁴ Present address: 25 Hammond Street, No. 1, Cambridge, MA 02138.

⁵ H. H. Wills Physics Laboratory, University of Bristol, Tyndall Avenue, Bristol BS8 1TL, England, UK.

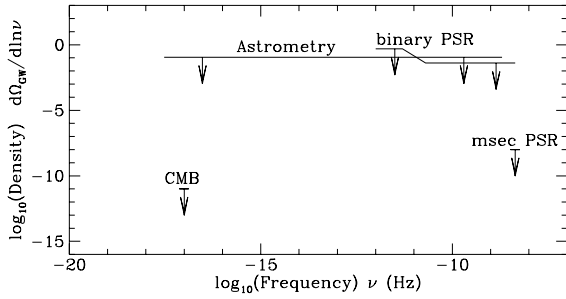


FIG. 1.—Limits on the spectrum of stochastic gravitational radiation, in units of closure density of the universe, per logarithmic spectral interval. Labels show the technique that yielded each limit: timing of millisecond pulsars (“msec PSR”; Backer & Hellings 1986; Kaspi et al. 1994; Thorsett & Dewey 1996), timing of binary pulsars (“binary PSR”; Bertotti et al. 1983; Taylor & Weisberg 1989; Thorsett & Dewey 1996), isotropy of the cosmic background radiation (“CMB”: Linder 1988a; Krauss & White 1992; Bar-Kana 1994), and the results of this paper (“Astrometry”). Because binary pulsar timing and astrometry yield constraints on the integrated energy density over a spectral range, their limits can be more stringent than shown, depending on the specific form of the spectrum.

1997), corresponding to observational limits on the energy density of gravitational waves of about that required to close the universe.

2. THEORETICAL BACKGROUND

Very long baseline interferometry (VLBI) measures positions of radio sources by measuring the difference in arrival times of their signals at antennas in different geographic locations (Shapiro 1976). The interferometrist assumes that the observations are made in a locally Minkowski reference frame (allowing for the orbital acceleration of Earth and the general relativistic light-bending of the Sun and planets) and so interprets these observations in the Gaussian normal reference frame. The delay T between arrival times measures the projection of the unit vector pointing toward the source onto the spacelike baseline vector that connects the antennas. Measurement of the delay for many sources on several baselines allows solution for both source positions and lengths and orientations of the baselines.

Pyne et al. (1996) describe the effect of a gravitational wave on a VLB interferometer: the wave produces variations in delay T , which are interpreted as variations in source position. A gravitational wave traveling toward $+z$, with the “+” polarization, produces metric perturbations $h \cos pt (\hat{x}\hat{x} - \hat{y}\hat{y})$ in the background coordinate reference frame, where h is the dimensionless strain of the wave, p is its angular frequency, and t is time. In the interferometrist’s Gaussian normal frame, the observed proper motion μ of a radio source at position (θ, ϕ) will be

$$\mu = \frac{1}{2}ph \sin p\eta \sin \theta (\hat{\theta} \cos 2\phi - \hat{\phi} \sin 2\phi). \quad (1)$$

Here θ measures the angle from $+z$, the direction of propagation of the wave, and ϕ measures the azimuthal angle around it, from the x -axis; the associated unit vectors on the sky are $\hat{\theta}$ and $\hat{\phi}$. Proper time in the Gaussian normal frame is η . We take h to be real and allow the origin of time η to express the phase of the wave. Figure 2 shows the pattern of proper motions that this gravitational wave produces.

The properties of this pattern of proper motions are not simple under rotation or superposition. However, the transverse vector spherical harmonics $Y_{l,m}^{(E,M)}$ form an orthonor-

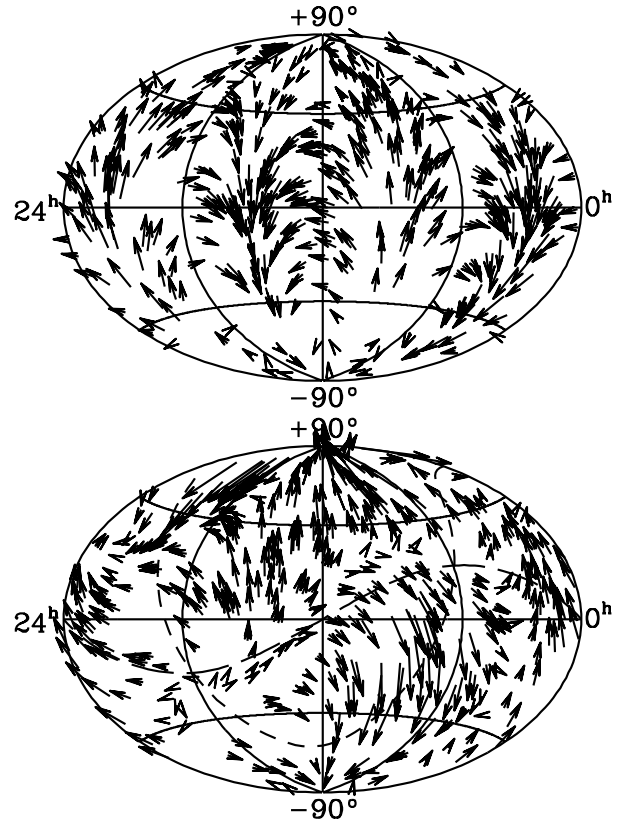


FIG. 2.—*Top*: Proper motions expected for a single gravitational wave. The metric perturbation is $h \cos [p(cz - t)] (\hat{x}\hat{x} - \hat{y}\hat{y})$, with \hat{z} toward declination 90° and \hat{x} toward right ascension 0^h . *Bottom*: Fitted coefficients of the second-order ($l=2$) transverse spherical harmonics, displayed as proper motions at locations of sources with measured proper motions. Arrow lengths in degrees equal proper motion in $\mu\text{as yr}^{-1}$. Coefficients are not shown for $l \neq 2$. Curves show the ecliptic (long-dashed curve) and Galactic (short-dashed curve) planes. The fitted coefficients are not statistically significant, so the observed pattern of motions is consistent with filtered noise.

mal basis for vector fields on a sphere, with well-understood behavior under rotation and superposition. Expanded in such harmonics, equation (1) takes the form

$$\mu = ph \sin p\eta \left[\frac{\sqrt{5\pi}}{6} (Y_{2,2}^E + Y_{2,-2}^E - Y_{2,2}^M + Y_{2,-2}^M) - \frac{\sqrt{70\pi}}{60} (Y_{3,2}^E + Y_{3,-2}^E - Y_{3,2}^M + Y_{3,-2}^M) + \dots \right]. \quad (2)$$

Here we use the convention of Mathews (1962, 1981) for transverse vector spherical harmonics. These fall into two categories, with one family, commonly denoted “poloidal,” “potential,” or “electric,” pointing down the gradients of scalar spherical harmonics and the other, known as “toroidal,” “stream,” or “magnetic,” pointing perpendicular to their gradients. We denote these categories as E and M , respectively (Mathews 1962, 1981), with the notation (E, M) meaning “ E or M .” Note that this $Y_{l,m}^M$ is the $X_{l,m}$ of Jackson (1975). Electric and magnetic harmonics are related by

$$\hat{r} \times Y_{l,m}^M = iY_{l,m}^E, \quad \hat{r} \times Y_{l,m}^E = iY_{l,m}^M. \quad (3)$$

Note that

$$Y_{l,-m}^E = (-1)^m (Y_{l,m}^E)^* \quad (4)$$

and that

$$Y_{l,-m}^M = (-1)^{m+1} (Y_{l,m}^M)^*, \quad (5)$$

where an asterisk denotes complex conjugation. The normalization condition is

$$\begin{aligned} 4\pi \langle Y_{l,m}^E (Y_{i,j}^E)^* \rangle &= 4\pi \langle Y_{l,m}^M (Y_{i,j}^M)^* \rangle = \delta_{li} \delta_{mj}, \\ \langle Y_{l,m}^E (Y_{i,j}^M)^* \rangle &= 0. \end{aligned} \quad (6)$$

Here angle brackets denote an average over the sky. Table 1 lists electric and magnetic vector spherical harmonics for $l \leq 3$.

Because the $Y_{l,m}^{(E,M)}$ form an orthonormal basis for vector fields on a sphere, they can represent proper motions due to a single wave, or any spectrum of waves. We use the expansion

$$\boldsymbol{\mu} = \sum_{l,m} (a_{l,m}^E Y_{l,m}^E + a_{l,m}^M Y_{l,m}^M) \quad (7)$$

to define the coefficients $a_{l,m}^E$ and $a_{l,m}^M$ in terms of the proper motion $\boldsymbol{\mu}$, observed over a small fraction of a gravitational wave period. The $a_{l,m}^{(E,M)}$ must satisfy

$$a_{l,m}^E = (-1)^m (a_{l,-m}^E)^*, \quad a_{l,m}^M = (-1)^{m+1} (a_{l,-m}^M)^* \quad (8)$$

(Mathews 1981), because $\boldsymbol{\mu}$ is real.

The squared proper motion averaged over the sky is related to the energy density of the wave T_{GW} by

$$\langle \mu^2 \rangle = \frac{1}{12} p^2 h^2 = \frac{8\pi}{3} \frac{G}{c^2} T_{\text{GW}}. \quad (9)$$

Here $\langle \mu^2 \rangle$ includes an average over many wave periods, as well as over the sky. Expansion of the mean square proper motion in vector spherical harmonics shows that $\frac{5}{6}$ of the mean square motion resides in the $l = 2$ harmonics:

$$\frac{1}{4\pi} \sum_m (|a_{2,m}^E|^2 + |a_{2,m}^M|^2) = \frac{5}{6} \langle \mu^2 \rangle. \quad (10)$$

Because the summed, squared moduli of the $a_{l,m}^{(E,M)}$ remain constant under rotation for each l , and for E - and M -harmonics separately, equation (10) holds for a gravitational wave propagating in any direction with any polarization.

If the phases, amplitudes, and directions of the many superposed waves in the spectrum are random at Earth, as is to be expected for a cosmological background of gravitational waves, the random-phase approximation shows that equations (9) and (10) will hold statistically, if $p^2 h^2$ is replaced by the integral $\int p^2 h(p)^2 d^3 p$, and if the average of the squared proper motion over time and sky is replaced by an average over an ensemble of gravitational wave spectra (see, e.g., Goodman 1985). Here $h(p)^2$ is the spectral density of the square of the dimensionless strain. Thus equation (10) shows that $\frac{5}{6}$ of the mean square proper motion due to the low-frequency gravitational wave background appears in second-order transverse spherical harmonics, and E - and M -harmonics contribute equally. We can express the energy density in such a stochastic background of gravitational waves as Ω_{GW} , its ratio to the closure density of the universe, $T_{\text{cl}} = 3c^2 H_0^2 / (8\pi G)$, and we can relate Ω_{GW} to proper motion in second-order transverse harmonics:

$$\Omega_{\text{GW}} = \frac{1}{H_0^2} \langle \mu^2 \rangle = \frac{6}{5} \frac{1}{4\pi} \frac{1}{H_0^2} \sum_{(E,M),m} |a_{2,m}^{(E,M)}|^2. \quad (11)$$

We seek to measure the $a_{2,m}^{(E,M)}$ and to thus measure, or set limits on, Ω_{GW} .

3. OBSERVATIONS AND DATA REDUCTION

We searched for the pattern expected for gravitational waves in proper motions of extragalactic radio sources. We estimated second-order spherical harmonics from a proper-motion solution using the US Naval Observatory comprehensive database of VLBI observations. This contains most of the suitable astrometric and geodetic observations of extragalactic radio sources made with the Mark III and compatible VLBI systems (Clark et al. 1985). Eubanks et al. (1997) describe the data analysis in detail; here we present a brief overview.

The database comprises 1,469,793 observations of delay T and its time derivative \dot{T} with different baselines and sources. The observations were made between 1979 August 3 and 1996 February 13, with more than 70% after 1990. Proper motions were determined for the 499 sources observed at more than one epoch. In fitting for the coeffi-

TABLE 1
VECTOR SPHERICAL HARMONICS

(l, m)	FACTOR	ELECTRIC $Y_{l,m}^E$ VECTOR COMPONENTS		MAGNETIC $Y_{l,m}^M$ VECTOR COMPONENTS	
		$\hat{\theta}$	$\hat{\phi}$	$\hat{\theta}$	$\hat{\phi}$
(1, 1)	$(3/16\pi)^{1/2} e^{i\phi}$	$-\cos \theta$	$-i$	1	$i \cos \theta$
(1, 0)	$(3/8\pi)^{1/2} \sin \theta$	-1	0	0	i
(1, -1)	$(3/16\pi)^{1/2} e^{-i\phi}$	$\cos \theta$	$-i$	1	$-i \cos \theta$
(2, 2)	$(5/16\pi)^{1/2} e^{2i\phi} \sin \theta$	$\cos \theta$	i	-1	$-i \cos \theta$
(2, 1)	$(5/16\pi)^{1/2} e^{i\phi}$	$1 - 2 \cos^2 \theta$	$-i \cos \theta$	$\cos \theta$	$i(2 \cos^2 \theta - 1)$
(2, 0)	$(15/8\pi)^{1/2} \sin \theta$	$-\cos \theta$	0	0	$i \cos \theta$
(2, -1)	$(5/16\pi)^{1/2} e^{-i\phi}$	$2 \cos^2 \theta - 1$	$-i \cos \theta$	$\cos \theta$	$i(1 - 2 \cos^2 \theta)$
(2, -2)	$(5/16\pi)^{1/2} e^{-2i\phi} \sin \theta$	$\cos \theta$	$-i$	1	$-i \cos \theta$
(3, 3)	$(105/256\pi)^{1/2} e^{3i\phi} \sin^2 \theta$	$-\cos \theta$	$-i$	1	$i \cos \theta$
(3, 2)	$(35/128\pi)^{1/2} e^{2i\phi} \sin \theta$	$3 \cos^2 \theta - 1$	$2i \cos \theta$	$-2 \cos \theta$	$i(1 - 3 \cos^2 \theta)$
(3, 1)	$(7/256\pi)^{1/2} e^{i\phi}$	$\cos \theta (11 - 15 \cos^2 \theta)$	$i(1 - 5 \cos^2 \theta)$	$5 \cos^2 \theta - 1$	$i \cos \theta (15 \cos^2 \theta - 11)$
(3, 0)	$(21/64\pi)^{1/2} \sin \theta$	$1 - 5 \cos^2 \theta$	0	0	$i(5 \cos^2 \theta - 1)$
(3, -1)	$(7/256\pi)^{1/2} e^{-i\phi}$	$\cos \theta (15 \cos^2 \theta - 11)$	$i(1 - 5 \cos^2 \theta)$	$5 \cos^2 \theta - 1$	$i \cos \theta (11 - 15 \cos^2 \theta)$
(3, -2)	$(35/128\pi)^{1/2} e^{-2i\phi} \sin \theta$	$3 \cos^2 \theta - 1$	$-2i \cos \theta$	$2 \cos \theta$	$i(1 - 3 \cos^2 \theta)$
(3, -3)	$(105/256\pi)^{1/2} e^{-3i\phi} \sin^2 \theta$	$\cos \theta$	$-i$	1	$-i \cos \theta$

NOTE.—From Mathews 1981.

TABLE 2
OBSERVED COEFFICIENTS OF TRANSVERSE HARMONICS

Parameter	Fitted Value ($\mu\text{s yr}^{-1}$)	Standard Error ($\mu\text{s yr}^{-1}$)
Acceleration: ^a		
\ddot{x}	1.9	6.1
\ddot{y}	5.4	6.2
\ddot{z}	7.5	5.6
Second-order transverse vector spherical harmonics: ^b		
$a_{2,0}^E$	12.1	16.6
$(1/\sqrt{2})(a_{2,1}^E - a_{2,-1}^E)$	-13.6	14.9
$(i/\sqrt{2})(a_{2,1}^E + a_{2,-1}^E)$	-21.7	15.6
$(1/\sqrt{2})(a_{2,2}^E + a_{2,-2}^E)$	4.2	12.5
$(i/\sqrt{2})(a_{2,2}^E - a_{2,-2}^E)$	-0.6	13.3
$ia_{2,0}^M$	1.7	14.4
$(i/\sqrt{2})(a_{2,1}^M - a_{2,-1}^M)$	17.8	15.0
$(1/\sqrt{2})(a_{2,1}^M + a_{2,-1}^M)$	-28.2	15.3
$(i/\sqrt{2})(a_{2,2}^M + a_{2,-2}^M)$	-17.6	13.9
$(1/\sqrt{2})(a_{2,2}^M - a_{2,-2}^M)$	10.7	15.0

^a Effects of acceleration of the solar system barycenter relative to the observed extragalactic radio sources correspond to first-order ($l = 1$) harmonics. Rotations also correspond to first-order harmonics; our fits included these but we do not report them, as they cannot be separated from Earth's rotation.

^b Second-order ($l = 2$) harmonics correspond to effects of low-frequency gravitational waves. Otherwise identical coefficients $a_{l,m}^{(E,M)}$ with opposite sign of m have been combined to reflect the fact that the fitted motions are purely real.

cients of transverse spherical harmonics, we used the 323 sources known to be extragalactic by their measured redshifts. Their mean redshift is 1.22.

Reduction of these data to source positions and proper motions follows standard procedures for astrometric and geodetic VLBI data (see, e.g., Clark et al. 1985). We removed the best models for (1) Earth orientation, tidal deformation, and location within the solar system, (2) atmospheric propagation, and (3) solar system effects of general and special relativity before fitting for proper motion. Simultaneous observations at two frequencies allowed calibration of the propagation delay through the ionosphere. The solutions for proper motions also included $\approx 400,000$ "nuisance" parameters, including those describing positions of sources and stations; clock behavior at different stations; optical path length through the atmosphere in a vertical direction and its horizontal gradients; unmodeled motions of Earth, including variations in rotation, polar motion, nutation, and precession; and gravitational deflection of light by the Sun (Eubanks et al. 1997). These nuisance parameters are chosen to have little covariance with source and station positions, and thus with proper motions. After the fit, the weighted root mean square of the scatters of the residuals in delay and in delay rate were 31 ps and 93 fs s^{-1} , respectively.

Effects of source structure and variations in atmospheric path length are among the expected systematic errors. The sources are highly energetic neighborhoods of active galactic nuclei. The well-known motions of jets from such sources can mimic proper motion, particularly in cases in which the stationary core component is weak or absent (see, e.g., Guirado et al. 1995). Such motions are expected to be many microarcseconds per year, but should not be correlated over the sky, so that they increase noise in the measurements but do not bias lower order transverse spherical harmonics. Atmospheric path length is removed via models

incorporating contemporaneous meteorological data, and the residual path length and its horizontal gradients are parameterized and estimated directly from the VLBI solution. Remaining atmospheric delay errors might show angular dependences that could mimic those expected for gravitational waves.

We then fitted transverse spherical harmonics to the measured proper motions. The fit minimized χ^2 , the summed, squared differences of proper motions, and the motions modeled by equations (7) and (8). These differences were weighted by the expected errors, given by the standard errors from the fit to delay and delay rate, scaled by a factor of 1.35, and with an assumed error added in quadrature (in each component of proper motion) of 30 $\mu\text{s yr}^{-1}$. This reweighting serves to make the χ^2 per degree of freedom about unity, as expected; it accounts, in particular, for effects of variations in source structure. Comparison of fits to subsets of the data suggested this scaling and addition in quadrature. Fits to subsets of the data did not change the fitted values significantly, although the standard errors increased.

The fit included coefficients for $l = 1$ transverse spherical harmonics, as well as the $l = 2$ harmonics characteristic of gravitational waves. The $l = 1$ M -harmonics correspond to a rotation, of no physical significance, as it is not separable from Earth's rotation; the $l = 1$ E -harmonics correspond to acceleration not included in models used for data reduction. This acceleration is an interesting cosmological parameter: it is sensitive to the Galactocentric acceleration of the solar system, as well as any acceleration of the Milky Way relative to distant quasars.

The measured values of the coefficients of second-order transverse spherical harmonics are statistically indistinguishable from noise. The residual χ^2 to the fit was 717, distributed among 627 degrees of freedom. Table 2 summarizes the results of the fit, and Figure 2 shows the results for the $l = 2$ harmonics in graphical form. The fitted coefficients are combinations of $a_{l,m}^{(E,M)}$ that satisfy equation (8) to produce real motions. The mild migration of sources away from the ecliptic in Figure 2 may reflect effects of the Sun on atmospheric propagation.

4. RESULTS

A particular value of Ω_{GW} corresponds to an ensemble of possible gravitational wave spectra and coefficients $a_{2,m}^{(E,M)}$. Equation (11) relates Ω_{GW} to the mean over the ensemble of the summed, squared coefficients. The measurement errors given in the last column of Table 2 also contribute to the measured $a_{2,m}^{(E,M)}$. We take these contributions into account to find the value of Ω_{GW} that yields summed, squared coefficients less than those we observe for only 5% of gravitational spectra and adopt this as our upper limit. This procedure includes effects of sample or cosmic variance. With 95% confidence, we find that $\Omega_{\text{GW}} < 0.11 h^{-2}$, where $H_0 = 100 h \text{ km s}^{-1}$. This limit holds for a stochastic spectrum of gravitational waves integrated over all frequencies less than half the inverse of the 10 year span of the observations, or about 2×10^{-9} Hz.

Considerable improvement in this limit should be possible over the next decade. The measurement accuracy for proper motions is proportional to the duration of observations to the 3/2 power. Because most data were acquired in the last 5–10 years, an additional decade of observing should improve the bound on Ω_{GW} by a factor of 3–8.

Moreover, we can reduce effects of source structure by choosing additional sources with little structure, from among the thousands observable astrometrically with the Very Long Baseline Array, and by using models derived from images of the sources to correct for effects of structure directly. Together, these improvements may be expected to

reduce the formal errors of measurements of Ω_{GW} by a factor of 10–100, within the next 10 years.

We thank J. Hartle for useful suggestions. This work was supported in part by the National Science Foundation (AST-9005038 and AST-9217784).

REFERENCES

- Backer, D. C., & Hellings, R. W. 1986, *ARA&A*, 24, 537
 Bar-Kana, R. 1994, *Phys. Rev. D*, 50, 1157
 Bertotti, B., Carr, B. J., & Rees, M. J. 1983, *MNRAS*, 203, 945
 Bondi, H. Pirani, F. A. E., & Robinson, I. 1959, *Proc. R. Soc. London A*, 251, 519
 Clark, T. A., et al. 1985, *IEEE Trans. Geosci. Remote Sensing*, 23, 438
 Durrer, R. 1994, *Phys. Rev. Lett.*, 72, 3301
 Eubanks, T. M., et al. 1997, in preparation
 Fabbri, R., & Pollock, M. 1983, *Phys. Lett. B*, 125, 445
 Fakir, R. 1994, *ApJ*, 418, 202
 Goodman, J. W. 1985, *Statistical Optics* (New York: Wiley)
 Grishchuk, L. P. 1993, *Phys. Rev. D*, 48, 3513
 Guirado, J. C., et al. 1995, *AJ*, 110, 2586
 Hogan, C. J. 1986, *MNRAS*, 218, 629
 Jackson, J. D. 1975, *Classical Electrodynamics* (2d ed.; New York: Wiley)
 Kaiser, N., & Jaffe, A. 1997, *ApJ*, 484, 545
 Kaspi, V. M., Taylor, J. H., & Ryba, M. F. 1994, *ApJ*, 428, 713
 Krauss, L. M., & White, M. 1992, *Phys. Rev. Lett.*, 69, 869
 Linder, E. V. 1988a, *ApJ*, 326, 517
 ———. 1988b, *ApJ*, 328, 77
 Mathews, J. 1962, *J. SIAM*, 10, 768
 ———. 1981, *Tensor Spherical Harmonics* (Pasadena: Caltech)
 Penrose, R. 1966, in *Perspectives in Geometry and Relativity*, ed. B. Hoffmann (Bloomington: Indiana Univ. Press), 259
 Pyne, T., Gwinn, C. R., Birkinshaw, M., Eubanks, T. M., & Matsakis, D. N. 1996, *ApJ*, 465, 566
 Rubakov, V. A., Sazhin, M., & Veriaskin, A. V. 1982, *Phys. Lett. B*, 115, 189
 Shapiro, I. I. 1976, in *Methods of Experimental Physics*, Vol. 12C, *Radio Observations*, ed. M. L. Meeks (New York: Academic), 261
 Taylor, J. H., & Weisberg, J. M. 1989, *ApJ*, 345, 434
 Thorsett, S. E., & Dewey, R. J. 1996, *Phys. Rev. D*, 53, 3468
 Vilenkin, A. 1981, *Phys. Lett. B*, 107, 47
 Zipoy, D. M. 1966, *Phys. Rev.*, 142, 825